CHAPTER 1

STM Imaging of the SnO$_2$ Surface

1.1 Introduction

Scanning tunneling microscopy (STM) can be used to resolve in real space the local electronic structure, and thus the atomic structure, of every kind of conducting solid surface [1]. Surface electronic and atomic structures determine the variety and nature of bonding environments, and the energetic pathways available to reactants as they adsorb, diffuse, and participate in surface reactions [2]. The use of scanning tunneling microscopy and atomic force microscopy (AFM) on metal oxide surfaces initially centered around the imaging of steps which often represent centers of catalytic activity. The density, orientation and in-plane topography of steps on solid surfaces can be resolved with STM without achieving lateral atomic resolution [1].

The primary focus of this experimental program was to be obtain atomic-scale images of SnO$_2$ following a variety of surface preparation techniques. The use of STM in the imaging of atomic structure of metal oxides is still in the preliminary stages with atomic-scale images being obtained in only a few cases. Early success has included the atomic-scale imaging of the TiO$_2$ (110) surface [3], the Fe$_2$O$_3$ (001) surface [2], and more recently the (4x1) reconstruction of the SnO$_2$ (110) surface [4] that was of interest in this study. Egdell and coworkers prepared the (4x1) reconstructed surface by ion bombardment with 1 keV Ar$^+$ and annealing at 700°C for 36 hours. The (4x1) SnO$_2$

(110) surface had a large number of periodic point defects which give rise to crisp (4x1) LEED pattern. Stable tunneling was obtained using a 1.5 V positive sample bias, similar to the +2.0 V bias used in imaging the TiO_2 (110) surface [3]. In contrast work on Fe_2O_3 (001) produced inconsistent results when tunneling at positive sample bias voltages [2]. STM images displaying arrays with O periodicity and others showing arrays with Fe periodicity were obtained at similar tunneling conditions, when positive bias voltages were used [2]. Consistent images were only obtained on Fe_2O_3 (001) at negative bias voltages where images showed a hexagonal array of O atomic sites with a 3-Å periodicity [2].

One goal of using STM to atomically image metal oxide surfaces lies in the potential to identify point defects on the surface and relate these defects to catalytic reactivity. The surface characterization techniques available previously, including low-energy electron diffraction (LEED) and ion scattering spectroscopy (ISS), are useful primarily in indicating long range order and are not always effective in identifying the number and type of point defects. STM, and to a lesser extent AFM, provide the opportunity for the first time to diagram individual atom positions to within a small fraction of an inner-atomic distance [5].

1.2 Experimental

All surface preparations and vacuum STM experiments were conducted in an ion pumped, single-chamber, stainless steel ultahigh vacuum (UHV) system. The Omicron Compact Lab UHV system is equipped with a focus cylindrical sector analyzer, a Omicron STM-1 with tripod scanner, a dual anode Mg/Al X-ray source for X-ray photoelectron spectroscopy (XPS), a Leybold differentially-pumped ion gun for Ar^+ and He^+ ion bombardment, a differentially-pumped helium UV lamp for ultraviolet photoelectron spectroscopy (UPS), and a set of Omicron 4-grid reverse view LEED optics. The base pressure of the UHV system is 7.5×10^{-11} Torr. Ion bombardment was performed at room temperature using 2 keV Ar^+ and 200 eV He^+. While in operation, the STM rested on vibration dampening springs with magnetic eddy current dampening.

Sample transfer in and out of the UHV system proceeds through a turbo-pumped load-lock chamber which is isolated from the main chamber of the UHV system with a manual gate valve. The load-lock chamber is vented and the sample is placed on the magnetically coupled introduction arm. A pressure of 5×10^{-9} Torr is obtained in the load-lock chamber, and then the sample is transferred to the main chamber manipulator using the magnetically coupled introduction arm.

A Digital Instruments Nanoscope III combined AFM/STM was used for air STM and all AFM experiments. Vibrational isolation was accomplished by placing the air STM in an acoustic dampening box suspended from a tripod with bungee cords. The sample was mounted directly to the base of the air STM using DAG, colloidal graphite suspended in iso-propanol, a conducting glue.

All STM images were collected in constant-current mode with the exception of

the atomic-scale images, less than 20 nm square, which were collected in constant-height mode. In constant-current mode a constant tip to sample separation is maintained with a feedback loop which ensures the average tunneling current is as close as possible to a user defined setpoint [6]. Information about the surface topography is obtained from the mechanical deflection of the tip. In constant-height mode, the tip travels in a horizontal plane above the sample and information about local topography and electronic structure is obtained from variations in the tunneling current [6]. Constant-height mode is advantageous for atomic-scale resolution imaging because it requires little mechanical response when imaging atomically smooth areas [2].

The synthetic SnO_2 sample used in this study was a piece of a larger crystal that was grown using the vapor phase transport method of Thiel and Helbig [7]. The resulting sample was approximately 4x7x1 mm^3. Additional experiments were conducted on a natural cassiterite sample, mineral form of SnO_2, from Usigodino, Spain which was obtained from the Geology Museum of Virginia Tech. The mineral sample had a large, macroscopically flat, natural growth face. SnO_2 natural growth faces are primarily (110) or (100) [6]. The natural SnO_2 sample was 9x8x1 mm^3. A Cu_2O (111) single crystal sample grown by a float zone technique [8] was also investigated briefly. The crystal was aligned using Laue back-scattering, and mechanically polished to within ±0.5° of the (111) face. The resulting sample size was 2x6x1 mm^3. Following mounting, the samples were rinsed with iso-propanol and placed in a vacuum drying oven at 150°C overnight before being introduced into the UHV system.

Two types of sample stubs were used to mount samples for experiments in the UHV system. The "resistive" sample stub consisted of a tantalum plate which provided

mechanical support and acted as an indirect heating source. The sample was held in place using two tantalum shims which were spot-welded onto the sample plate. The sample was heated resistively using ceramically isolated molybdenum wire located on the main chamber manipulator. The molybdenum wire was located approximately 0.5 cm below the bottom surface of the sample stub, when the sample stub was placed in the manipulator. A thermocouple was located just above the surface on one side of the "resistive" sample plate which provided an approximation of the sample temperature. A maximum annealing temperature of approximately 750°C was obtainable using the "resistive" sample stub. At the maximum temperature the sample stub was a uniform red hot.

The "direct" heating stub allowed the sample to be in direct contact with a hot metallic filament. The sample was heated resistively by passing a current through a metallic filament that was mounted under the sample. A number of different metallic filaments were tried including tantalum plates and molybdenum foils. The tantalum plates ranged in thickness from 0.3 mm to 1.0 mm with an average width of 0.7 cm, approximately the same width as the samples. The tantalum plates provided enough mechanical support, but they did not allow heating to high enough temperatures. The tantalum plates were only a dull red hot at the maximum power output. A 0.1 mm thick molybdenum foil was used with filament widths ranging from 0.4 cm to 1.0 cm. The molybdenum foil could be heated to a bright yellow color. The intensity of the light depended on the foil width and power output. The molybdenum foil did not however provide sufficient mechanical support as it would consistently break during the annealing process. The filament would break after five minutes, or less at the maximum power of

10-20 amps. A double layer of foil with a width of 0.5 cm was tried, however it still did

not provide sufficient mechanical support with the filament breaking after three minutes.

A single layer of molybdenum foil was consistently used with the direct heating stub

because of its ability to reach significantly higher temperatures than any of the tantalum

plates. The heating would end abruptly with the breaking of the filament resulting in wide

variations in the annealing time from five minutes to less than a minute.

The main disadvantage of the "direct" heating stub was the lack of a thermocouple

to at least approximate the sample temperature. The "resistive" sample stub allowed the

temperature to be estimated with a thermocouple located at the base of the sample plate.

In the "direct" heating stub the filament and sample were raised approximately one

centimeter off the sample plate. The existing thermocouple could no longer be used to

accurately estimate the sample temperature. The sample temperature was qualitatively

estimated from the brightness of the metallic filament during annealing [9].

1.3 <u>Results and Discussion</u>

1.3.1 Synthetic SnO$_2$ Sample

The STM work can be divided into two primary phases. The first phase involved the use of a synthetic SnO$_2$ sample and the second phase involved a natural SnO$_2$ sample from that was obtained from the Geology Museum at Virginia Tech. Additionally, approximately a weeks worth of work was conducted on a single crystal synthetic Cu$_2$O (111) sample. All surface preparations were conducted in UHV with the STM imaging being divided between air and UHV conditions. Experimental progress was slowed due to a high demand for time on the UHV system, which allowed only one week of experimental time per month.

Initial experiments were conducted using the synthetic SnO$_2$ sample with the "resistive" sample stub. The surface of the SnO$_2$ sample was prepared by sputtering with 2 keV Ar$^+$ for 30 minutes and annealing for 2-3 hours at a thermocouple reading of 750°C. A total of three cycles of ion bombardment and annealing were completed. The LEED pattern was checked when the sample was introduced into the chamber and after each cycle of sputtering and annealing. Bright spots were observable on the LEED pattern, but the presence of a high diffuse background made it impossible to determine the periodicity. The quality of the LEED pattern did not improve over the course of the three sputtering and annealing cycles.

The sample was removed from vacuum even though the long range order of the sample had not been established by LEED. The Nanoscope III STM was used to image the sample in air following the UHV treatment. A Platinum/Iridium tip was used for all

the experiments on the air STM. Bias voltages ranging from +0.0 V to +5.0 V were attempted. The positive bias voltage indicates a positive sample bias with electrons traveling from the Pt/Ir tip to the sample. Stable images were obtained at a bias voltage of +2.0 V. The general roughness of the surface was visible in a series of images ranging in size from 1000 nm to 42.3 nm. Two examples from this series of images are shown in Figures 1.1 (a,b).
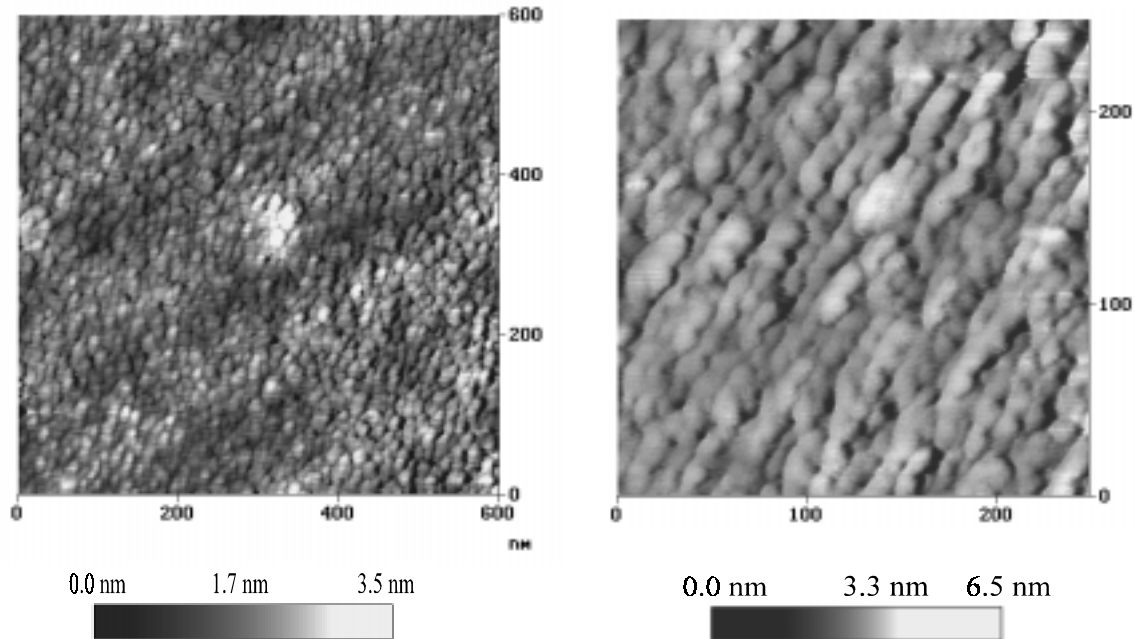

Figure 1.1: (a) 600 nm x 600 nm and (b) 250 nm x 250 nm STM images of the synthetic SnO₂ sample obtained at a sample bias of +2.0 V and a 0.14 nA tunneling current. Both images were collected in constant current mode.

The roughness was associated with a large number of small features, with an average height of approximately 3 nm, rather than more significant terraces. A maximum of 4.0 nm of roughness was observed over a 130 nm square scanning area. The mounds appear to have some order with alignment in diagonal rows across the images. These images were consistent with other images obtained on subsequent days following similar surface preparation. Images obtained on TiO_2 (110) were similar to the images seen during this

initial phase [3]. Atomic scale resolution was obtained on the TiO_2 (110) surface only after annealing to higher temperatures which resulted in the formation of long flat terraces in place of the smaller uneven mounds seen previously. It was hoped that the SnO_2 surface would behave similarly so work was begun to determine a way to increase the sample annealing temperature.

Work was continued on the synthetic single crystal SnO_2, now using the "direct" heating stub. Thin molybdenum foil filaments, with an average width of 0.7 centimeters were used. A number of sputtering and annealing cycles were conducted where the sample was sputtered with 2 keV Ar^+ ions for 30 minutes and then annealed to a yellow hot filament brightness. In each case the molybdenum filament broke after an annealing time ranging from 1-5 minutes, at the maximum power output of 10 amps. The annealing temperatures varied based on slight variations, ± 0.2 cm, in the width of the molybdenum foil. An annealing temperature of 1200 K - 1500 K can be estimated from the brightness of the molybdenum filament [9]. The temperature was estimated using a blackbody approximation accounting for significant deviation from ideal blackbody behavior with the molybdenum filament. Differentiation of the temperatures was limited by my ability to identify variations in the brightness of the glowing filament. A number of pressure spikes occurred during the annealing cycles lasting from 30 seconds to a couple of minutes. During these pressure spikes the pressure increased from 1-4 x 10^{-9} Torr to pressures in the range of 4-8 x 10^{-7} Torr. Viewing the sample under a microscope revealed that fluid/gas inclusions from the bulk had burst out of the surface. The bursting inclusions were likely responsible for the pressure spikes observed during annealing. The sample was discolored after heating to these higher temperatures taking on a noticeable

11

clouded tint.

Following the high temperature treatments the central portion of the sample was no longer conductive enough for STM imaging. A wide range of bias voltages were attempted, in 1 V increments, between -10 V and +10 V, none of which resulted in an engagement between the tip and the sample. A tungsten tip was tried in addition to the Pt/Ir tip used previously. Tunneling was possible near the ends of the sample, but only at high positive bias voltages in the range of 8-10 V. The higher conductivity at the ends of the sample may have been the result of a non uniform temperature distribution with lower temperatures near the shims. The conductivity may also be caused by the deposition of impurities on the sample as a result of contact with the shims. Under these conditions the tunneling was very unstable with the tip consistently exceeding the z-limit and drifting off scale. No images were obtained which accurately detailed the surface topography of these areas.

The sample was removed from vacuum and imaged using AFM to see if the surface topography had undergone any structural changes. AFM has the advantage of not requiring a conductive sample, however it is not as well suited for obtaining atomic-scale resolution. Larger features appeared on the surface although they lacked the uniformity of a well-ordered stepped surface. The surface was smoother with a reduction in the height of the features from a maximum of 8 nm prior to the high temperature treatments, to a value of only about 1.5 nm, over a 432 nm square scan area. The changes in the surface are shown in Figure 1.2 (a,b), where an STM image of the surface prior to using the "direct" heating stub and an AFM image following a series of high temperature treatments are shown.
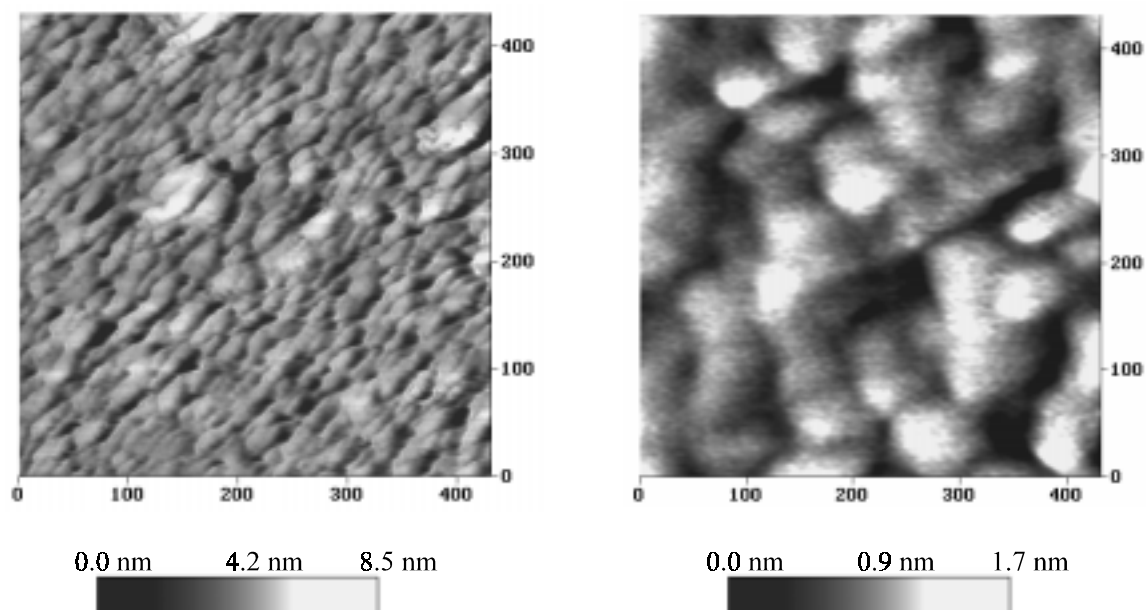
0.0 nm　　4.2 nm　　8.5 nm　　　　0.0 nm　　0.9 nm　　1.7 nm

Figure 1.2: (a) 432 nm x 432 nm STM image of the synthetic SnO₂ sample obtained at a sample bias of +2.0 V and a 0.18 nA tunneling current. The image was collected in constant current mode. (b) 432 nm x 432 nm AFM image of the synthetic SnO₂ sample obtained following a series of high temperature treatments.

The synthetic SnO_2 surface appeared to be moving from the extremely rough surface to the smoother terraced surface that was observed for TiO_2 (110) [3].

A new electrical feedthrough was purchased which allowed the current that was supplied to the "direct" sample stub to be doubled to 20 amps. A molybdenum foil filament that was approximately 25% wider than the sample, 0.9 cm, was used. The wider molybdenum filament would break at higher amperages usually between 15 and 20 amps. At the maximum power output the molybdenum filament was an extremely bright yellow, that was impossible to look at for more than a few seconds. The filament generally broke after an annealing time of two minutes or less at the maximum power output. After each sputtering, 2 keV Ar^+ for 30 minutes, and annealing cycle STM was attempted in vacuum. A number of different tunneling conditions were tried including positive and negative bias voltages (-10 V to +10 V), and Pt/Ir and tungsten tips. The

conductivity of the central part of the sample remained too low for STM imaging. No images were obtained that accurately detailed the surface topography, even on a large scale.

The loss of conductivity with higher annealing temperatures is not a completely unexpected result. An increase in the O:Sn ratio, and the accompanying decrease in conductivity, has been observed on ion-bombarded SnO_2 (110) over a range of annealing temperatures from 700-1000 K [10]. Annealing temperatures as high as 1500 K were used in these experiments. It is possible that the higher annealing temperatures increased the rate of oxygen diffusion from the bulk to the surface, resulting in a significant reduction in surface conductivity by reoxidizing in-plane vacancies.

1.3.2 Natural SnO$_2$ Sample

The second phase of the study involved a natural SnO_2 sample with a large natural growth face. No detectable LEED pattern was observable for the as-inserted natural SnO_2 sample, only diffuse background. Two cycles of sputtering and annealing were conducted. The sample was sputtered for 15 minutes using 200 eV He$^+$ and annealed at 750°C for 5 minutes. The LEED pattern was checked at the conclusion of the two cycles with no detectable pattern present. The sample was conductive enough to do STM in air over a wide range of bias voltages, -5 V to +5 V. The surface was extremely rough, with a maximum of 15 nm of relief over a 500 nm square scanning area. Stable imaging was achieved with positive bias voltages in the range of 1-2 V. Further surface treatment appeared necessary to smooth the surface and create long range order.

The natural sample was trimmed while still preserving the natural growth face,

allowing it to be mounted in the "direct" heating stub. The sample was placed in the UHV system and ion bombarded with 2 keV Ar^+ for three hours. During annealing the molybdenum filament was heated to a yellow hot where it remained for 20 minutes before breaking. A wider filament, approximately 0.9 cm, was used which allowed the annealing to continue for an extended amount of time. The annealing temperature was not as high as some of the temperatures achieved with the synthetic SnO_2 sample. A rectangular (1x1) LEED pattern was observed after the sample sat overnight. The LEED pattern was not crisp, but it was significantly better than anything achieved previously on the synthetic or natural samples. The sample appeared smoother based on a series of moderate quality images collected with the STM under UHV conditions. A roughness of approximately 3 nm was observed over a scanning area of 50 nm square. The surface topography contained large circular features. The features were not extremely uniform with the topography resembling the AFM images obtained on the non-conductive synthetic SnO_2 sample (Figure 1.2 (b)). A tungsten tip was used in collecting these STM images. The quality of the LEED pattern and the STM images may have been limited by the fact that the sample sat overnight in the UHV system prior to being imaged. As a result of the broken filament, the sample could not be annealed after sitting overnight, leaving a layer a adsorbed gases on the surface which are usually removed with heating. Even under UHV conditions, with a background pressure was in the range of 10^{-9} Torr a significant amount of adsorption can occur from the primary background gases including H_2O.

A slightly wider molybdenum filament, approximately 1 cm, was used once again with the hope that it would not break as easily and allow the sample to be imaged on a

number of consecutive days, without being removed from the vacuum system. The sample was sputtered with 2 keV Ar^+ for 30 minutes and then annealed until the filament was yellow hot. The filament did not break following annealing for five minutes at the maximum output of 20 amps. The cycle of sputtering and annealing was repeated the following day without removing the sample from UHV. The second day the filament broke following two minutes at the maximum annealing temperature. STM images were collected each day following the sample preparations. STM was used to identify a rough spot and in contrast a relatively flat spot over a range of 400 nm. Imaging was continued over the flat area with quality images being collected over areas between 100 nm and 400 nm square. The surface topography consisted of large mounds unevenly distributed over the surface. Tunneling conditions included a positive sample bias of 2.0 V and a setpoint current of 1.0 nA, using a tungsten tip. The gain ranged from 7.0% over a 400 nm scanning area to 4.5% for a 100 nm area. Below 100 nm the quality of the images was significantly reduced losing a lot of the detail seen previously in the larger images.

The natural sample was annealed to 750°C for five minutes. A new Pt/Ir tip was placed in the vacuum STM. Images were collected ranging in size from 400 nm to 3.0 nm square. An example from this series of images is shown in Figure 1.4(a). The atomic-scale images, less than 20 nm, represented the first time reproducible atomic-scale "features" were observed. The atomic-scale "features" primarily consisted of mounds with a separation of 3-4 Å which were observed only over small areas, less than 20 Å. This 3-4 Å separation is comparable to the expected O periodicity in the [001] direction, 3.19 Å, for (1x1) SnO_2 (110) surfaces. A ball model illustration of the ideal stoichiometric SnO_2 surface is shown in Figure 1.3.
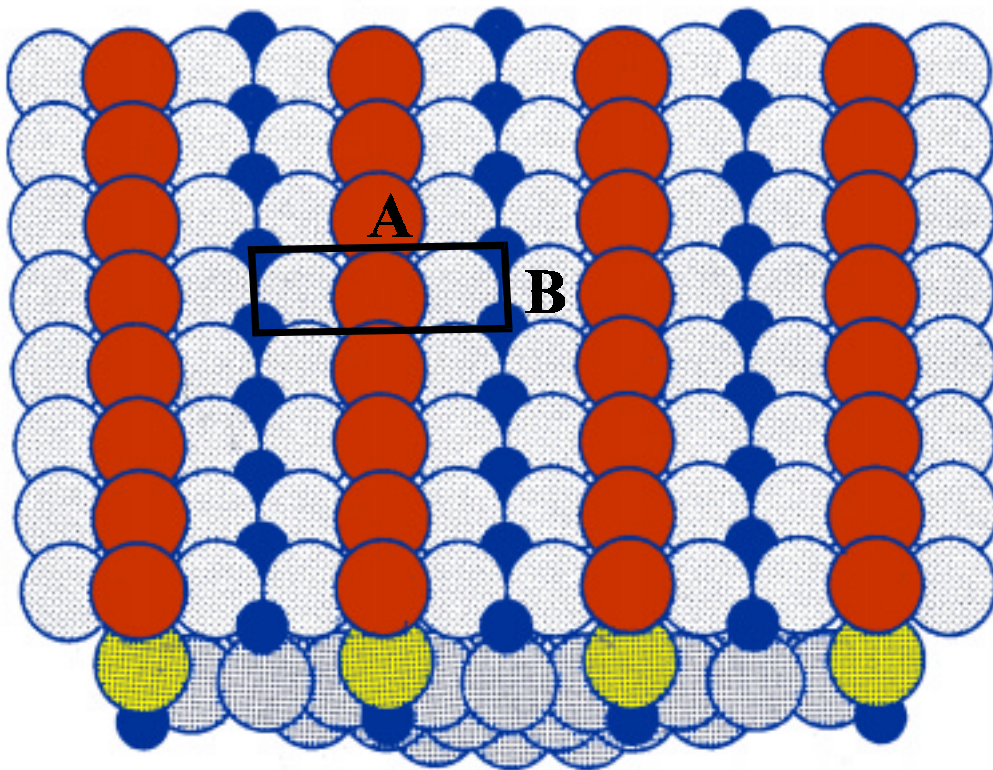
Figure 1.3 : Ball model illustration of the ideal stoichiometric SnO$_2$ (110) surface. The unit cell is 6.70 Å (A) by 3.19 Å (B).   Small circles represent Sn cations, larger circles represent O anions.

Figure 1.4 (b) shows an enlargement of a 16 Å square section of Figure 1.3 (a) which includes a number of atomic scale mounds. The approximate separation between two mounds is indicated with a line in Figure 1.3 (b). A more accurate estimate of the mound separation could not be obtained due to sample roughness and image interference. Interference is prominent when imaging at high bias voltages and gain values, such as these, on an atomic-scale. Smoothing and filtering routines, often used to clarify atomic position, were not able to generate a clearer image because of the extent of surface roughness. A unit cell could not be identified due to the small scan area that was atomically resolved and the variations in the atomic topography.
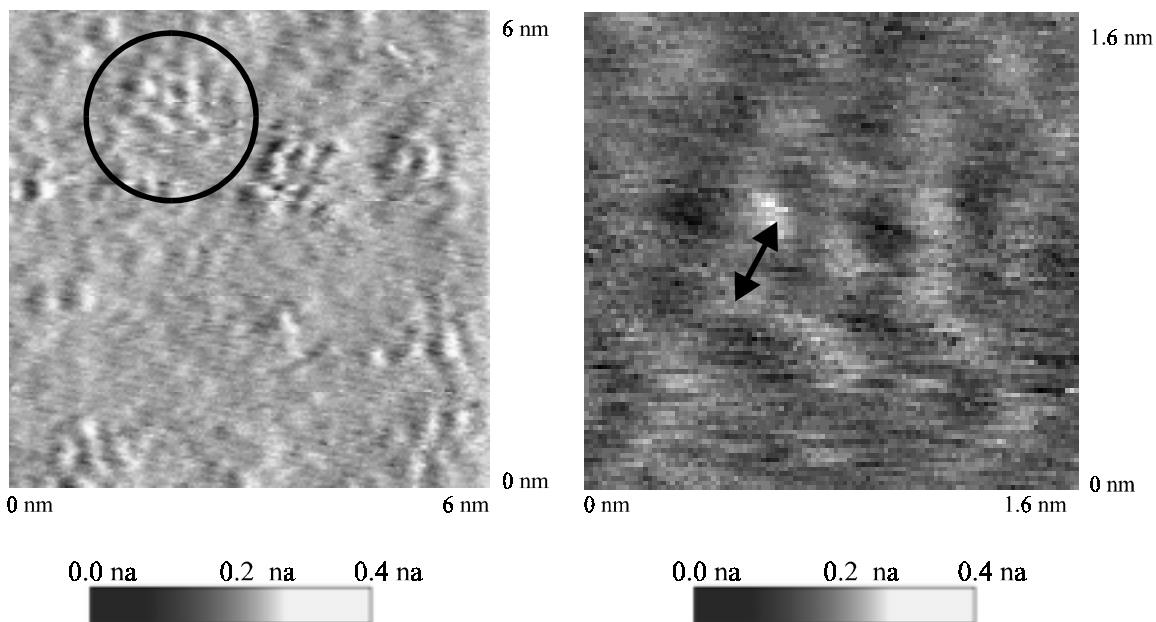
Figure 1.4: (a) 6.0 nm x 6.0 nm STM image of the natural SnO$_2$ sample obtained at a sample bias of +2.0 V and a 0.4 nA tunneling. Image was collected in constant height mode. (b) 1.6 nm x 1.6 nm enlargement of an area from Figure 1.3 (a).

These atomic-scale images were collected at a bias voltage of +2.0 V and a setpoint current of 0.3 to 0.4 nA. The gain ranged from 2.8% to 4.0% over scanning sizes of 3.0 to 6.0 nm square. Atomic scale images were obtained following annealing to 750°C for five minutes without ion bombardment. Previously the sample had undergone a number of cycles of sample cleaning with 2 keV Ar$^+$ and high temperature, 1200-1500 K, treatments before being removed from vacuum and placed on the "resistive" stub for the final annealing to 750°C. This set of images represented the first time a Pt/Ir tip had been used in vacuum to image the natural SnO$_2$ surface. The atomic-scale images were interesting because they were the first images collected on this scale which included reproducible "features", in this case small areas of evenly spaced mounds, that were not overshadowed by interference. The images did not provide information with regard to atomic position on the surface, but they do provide a measure of hope for future work in

this area.

The (4x1) reconstruction of the SnO_2 (110) surface that was atomically imaged by Egdell and coworkers was obtained following ion bombardment with 1 keV Ar^+ ions and annealing at $700^\circ C$ for 36 hours [4]. In the current study annealing times were significantly shorter, ranging from 1-20 minutes, over an estimated temperature range of 1000 K to 1500 K. On TiO_2 (110) a well-ordered, stepped surface was obtained after flashing the sample to 1200 K for five seconds [3]. A longer annealing time, instead of higher annealing temperature, may of been required to achieve a well-ordered, terraced SnO_2 surface, that is conducive to atomic-scale imaging. Stable images were obtained on SnO_2 surfaces only at positive sample bias voltages. A positive sample bias voltage of 1.5 V was found to be optimal in achieving stable tunneling and unit cell resolution for the (4x1) reconstruction of SnO_2 (110) [4]. In this study a positive sample bias voltage of 2.0 V proved optimal in imaging the synthetic and natural SnO_2 samples.

1.3.3 Single Crystal Cu_2O (111) Sample

One attempt was made at imaging the Cu_2O (111) surface. No detectable LEED pattern was observable for the as-inserted Cu_2O (111) sample, only diffuse background. The sample was ion bombarded with 2 keV Ar^+ for 15 minutes and then annealed to 750°C for five minutes. The quality of the LEED pattern did not significantly improve following sample preparation. The vacuum STM was used to collect a series of images, using a tungsten tip, varying in size from 20 nm to 1000 nm, over a range of bias voltages from -3.0 V to +3.0 V. An example from this series of images is shown in Figure 1.5. The most stable imaging was obtained at a negative sample bias voltage of 3.0 V and a

tunneling current of 0.6 nA. The surface appeared very rough with a maximum of 4.5 nm
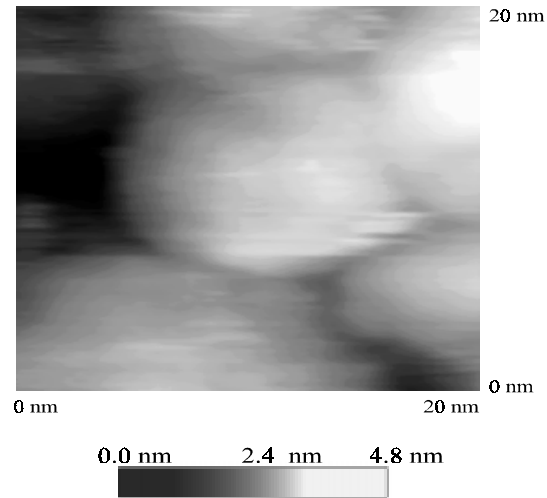
of relief over a 20 nm scan area.

Figure 1.5: 20 nm x 20 nm STM image of the single crystal Cu₂O (111) sample obtained at a sample bias of –3.0 V and a 0.6 nA tunneling current. The image was collected in constant current mode.

1.4 Conclusions

No atomic-scale images were collected on the SnO_2 or Cu_2O surfaces which provided information regarding atomic positions and point defects on the surface. The SnO_2 surface appeared to flatten considerably, with large unevenly distributed circular features forming following high temperature treatments of up to 1500 K. The conductivity of the synthetic SnO_2 surface was significantly reduced following annealing at temperatures of approximately 1200-1500 K, making tunneling impossible. A decrease in conductivity was not observed for the natural SnO_2 sample following similar high temperature treatments, most likely due to impurities which act as dopants.

1.5 <u>References</u>

[1]   C. J. Chen, <u>Introduction to Scanning Tunneling Microscopy</u> (Oxford University Press, New York, 1993).

[2] C. M. Eggleston, M. F. Hochella, *American Mineralogist* **77** (1992) 911.

[3] G. S. Rohrer, V. E. Henrich, and D. A. Bonnell, *Surface Science* **278** (1992) 146.

[4] F. H. Jones, R. Dixon, J. S. Ford, R. G. Egdell, and J. B. Pethica, *Surface Science* **376** (1997) 367.

[5] V. E. Henrich and P.A. Cox, <u>The Surface Science of Metal Oxides</u> (Cambridge, New York, 1994).

[6] R. Howland and L. Benator, <u>A Practical Guide to Scanning Probe Microscopy</u> (Park Scientific Instruments, 1993).

[7] B. Thiel and R. Helbig, *J. Cryst. Growth* **32** (1976) 259.

[8] A. Many, Y. Goldstein, and N. B. Grover, <u>Semiconductor Surfaces</u>, (North Holland, Amsterdam, 1971).

[9] K. Nassau, <u>The Physics and Chemistry of Color</u>, (John Wiley and Sons, New York, 1983).

[10] D. F. Cox, T. B. Fryberger, and S. Semancik, *Surface Science* **224** (1989) 121.